25th ABCM International Congress of Mechanical Engineering
October 20-25, 2019, Uberlândia, MG, Brazil

COB-2019-1994
EVALUATION OF A PERPENDICULARITY METHODS FOR A ROBOTIC END EFFECTOR IN A CURVED SURFACE APPLICATION TO THE AIRCRAFT INDUSTRY

Kleber Roberto da Silva Santos
UNIFEI – Universidade Federal de Itajubá – 1303 BPS Ave, Itajubá,/MG, 37500-909, Brazil
santoskr@unifei.edu.br

Gustavo de Melo Carvalho
Rodrigo Tanure Tricarico
Luiz Fernando L. Rocha Ferreira
Emília Villani
ITA – Instituto Tecnológico de Aeronáutica – 50 Marechal Eduardo Gomes Square, São José dos Campos/SP, 12228-900, Brazil
gumelo@ita.br; rodrigotanure@ccm-ita.org.br; luiz.ferreira@ccm-ita.org.br; evillani@ita.br

Abstract. *In this paper, we present, compare and analyse the results of two different solutions for correction of the perpendicularity error of industrial robot manipulator end effector and curved surfaces, one of which uses an algorithm already developed for flat surfaces that will be tested with few modifications for its efficiency for curved surfaces. In the new approach the robot's pose is normalized through a linear sensor that allows us to quickly generate the correction angles and the Z distance, this is done in two different directions, allowing us to generate correction angles B and C in relation to surface. The main focus of this work is to evaluate the methods presented within a maximum error of 0.5 degrees between the manipulator and the normal of the table tested, and to verify the influence of different sensors used in the first method. The flat surface results did not satisfied the requirement of* 0.5^o*, but the following tests on tubular and spherical surface proved the reliability of the method on curved surfaces and achieved median result around* 0.1^o*. This work is related to the projects of the Center for Competence in Manufacturing (CCM), under development at ITA, in partnership with Embraer and supported by FINEP.*

Keywords: *automation, perpendicularity, design of experiments, end effector, measurement system.*

1. INTRODUCTION

The robotics use in the industry has been growing exponentially since the last industrial revolution mainly due to the great demand for products made quickly and with high quality. Industrial robots can be found in many different sectors of manufacturing, capitally in the automotive industry which produces thousands of cars daily. On the other hand, the aerospace industry produces only a few dozen units per day which shows why there aren't so many robotic arms in their production. However, as this branch of industry is focused on the highest quality of its products, this reality is changing rapidly.

Therefore, the search for automation process has been one of the main objectives among aeronautical industries, in order to reduce production cost. This scenario motivated the development of researches to get around limitations related to the application with robots in this branch (Furtado *et al.*, 2009).

There are many applications in which it's necessary to reach the perpendicularity of the robotic arm end effector. For instance, this recent research chose the drilling process as one of the most suitable to automate. Based on the high number of drilling process on a single airplane, the research by (Cibiel *et al.*, 2006) showed that even though not many units are produced annually, the automation of this particular process is worth.

Many studies show that perpendicularity has an important role in the quality of the screw holes, affecting its fatigue life (Liu *et al.*, 2007). In turn, the fatigue accidents are usually caused by joint positioning error (around 70%) and the fatigue cracks come from riveting holes (around 80%). An experiment carried out from a titanium alloy showed that the fatigue life would reduce by 47% if the riveting holes were tilted above 2 degrees (Gao *et al.*, 2017). The fatigue life of the major components can be determined mainly by the design of geometric details, such as tightening screws and filleting, which are the main stress zones. During the last decades, many improvements have been made to improve the quality of the holes, which have resulted in a better understanding of the fatigue and fracture behavior of materials for the

aeronautics industry, as well as new manufacturing techniques and good design practices (Gao *et al.*, 2015).

Thus, it is possible to verify that the perpendicularity of the end effector of an industrial robot for processes like drilling and riveting has an extreme importance in the airplane's lifespan.

In this paper we discuss the evaluation of two perpendicularity methods, similarly presented in (Santos *et al.*, 2018), with a few modifications. The modificated methods ensure the applicability not only on flat surface, but on curved surface too. The curved surfaces to be tested will be either with one-way curvature characterizing a cylinder or with two-way curvature forming a sphere or elliptical cap.

Using the static method proposed in (Santos *et al.*, 2018), necessary changes were made to adapted the normalization on curved surfaces, which, besides being the most common in the aeronautic industry, are those that present a more critical situation to guarantee the surface normalization and to perform the drilling process. In order to perform such an operation, the same equipment as in (Santos *et al.*, 2018) will be used in order to generate data that allow us to analyze its efficiency in relation to the flat surface methods.

A robotic end-effector with two laser sensors Fig.1, a laser scanner Fig.1b and a single point Fig.1a, was designed and coupled to the end effector of the KUKA robot, the LBR IIWA 14 R820, in order to perform the algorithms developed for aeronautical applications that require perpendicularity between the effector and the work surface. For this verification, a design of experiments was done to determine which algorithm is most suitable within a 0.5^{o} deviation range between the normal work surface and the end effector.

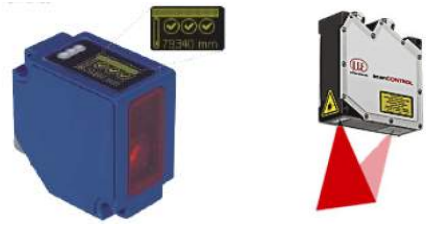

(a) Single point Sensor. (b) Laser scanner Sensor.

Figure 1: Sensors used.

2. METHODOLOGY

For the evaluation of both methods, the disposition and equipment are the same as described in Santos *et al.* (2018), showed in Fig. 2. The KUKA LBR IIWA 14 is a 7DOF industrial robot, with two sensors mounted on its end-effector. The first sensor is a point distance measuring, model OCP662P0150E from Wenglor and the second is a 2D laser scanner sensor from Micro Epsilon, model LLT26-100.

(a) Flat Surface. (b) Spherical Surface. (c) Tubular Surface.

Figure 2: Test surfaces of perpendicular algorithms.

One of the proposed evaluation methods for testing curved surfaces is the static method described in Santos *et al.* (2018) with some modifications. This method consists of evaluating a projected line on the surface from the 2D scanner, where its slope represents the correction angle. The other correction angle is calculated using a point of the scan sensor and the point sensor to project a second line in the plane and thus calculate the correction. This algorithm is described in detail in Santos *et al.* (2018) and will be evaluated using a flat surface Fig. 2a and compared to the modified algorithms for analysing curved surfaces, as seen in Fig. 2b and Fig. 2c .

The two methods of perpendicularity analysed in this work are called Static Method (Santos *et al.*, 2018) and Semi-Static Method,this name is get because it is a variation of the Static Method, which uses 2D scan to generate a projection on the surface. In the Semi-Static Method, the end-effector of the robotic manipulator is rotated to trace this projection in two distinct directions.

The end-effector used in the application during each of the proposed methods has been designed to ensure that both sensors are aligned in the same plane, thus minimizing the errors that are entered by the effector's manufacture. It was modelled using a 3D printing machine, as you can see in Fig. 3.

Figure 3: End-effector

Finally, a measurement system was used as a reference for the method evaluation. The equipment used was a laser tracker model Leica AT960, as can be seen in Fig. 4. Acquisition of data generated as a point cloud is interpreted using Poliworks software, which creates a CAD model of the scanned surface.

Figure 4: Laser tracker Leica model AT960.

2.1 Algorithms

This section will present the algorithms used in detail. Introducing the basis of calculations and software used for the study in question.

2.1.1 Parabolic Static Method Algorithm

It is called static due to the lack of any movement, but the end-effector pose correction to work. To execute this algorithm, the point sensor and the scan sensor are used in order to calculate the normal vector of the robotic end-effector in relation to the target surface. The line projected on the curve surface by the laser beam from the scan sensor generates a point cloud, in which each point has a value of x and z in the sensor frame reference (X_s,Z_s), that is better fitted to a parabola. The parabola equation is derived resulting into a line equation Z. Another line can be calculated with the point projected by the point sensor and the center point of the line projected by the scan sensor so α can be calculated. The correction angles α (Fig. 5b) and β (Fig. 5a), which are the arc tangent of the line coefficient, are calculated the same

way as discussed on the previous paper (Santos *et al.*, 2018) therefore will not be detailed on this work. The correction angles can be found by applying the equations eq. 1, eq. 2 and eq. 3.

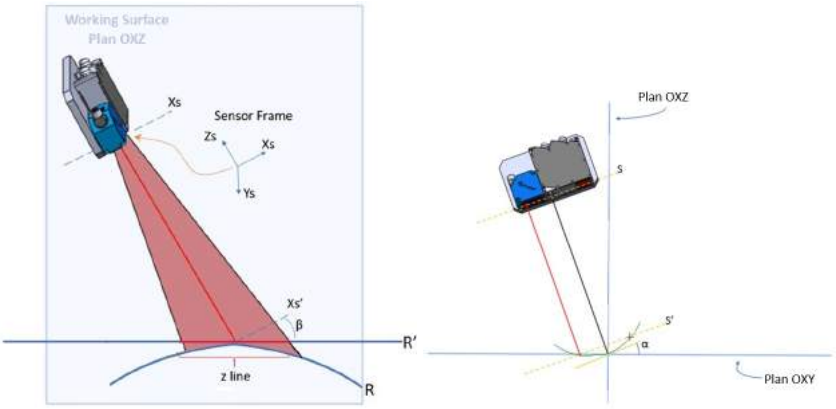

(a) Angle β in scan line projection. (b) Angle α in scan line projection.

Figure 5: Correction angles on curved surfaces.

$$z = mx + b \tag{1}$$

$$\arctan(m) = \beta \tag{2}$$

$$\arctan(Z_{point} - Z_{scan}/(20 - 0)) = \alpha \tag{3}$$

Where m and b are the angular and linear coefficients, respectively.

2.1.2 Semi-Static Method Algorithm

On the Semi Static Method, the scan sensor emits a laser beam on the surface and acquire a point cloud data represented as white dots on Fig. 6a, in which each point has a value of x and z in the sensor frame reference (X_s,Z_s). This data is passed to an already embedded fit-curve feature on Labview to adjust these points to a parabola 'W' represented as the green line on Fig. 6a. Once the curve equation is known, its derivative is calculated in point X equal to 0 since the center point of the laser beam is aligned with the TCP's origin of the the end-effector. The result is a line Z, tangent to the target point represented as the blue line on Fig. 6a and its equations on Fig. 6b. Then the robot rotates 90^{o} on the Z_s axis of the scan sensor and repeat the process above generating another line. The lines are called Z_1 and Z_2.

Similarly, as explained on the static method, the end-effector will only be perpendicular to the work surface if the angle β and α are equal to 0. Therefore, the correction angles are the arc tangent (Eq. 5 and 7) of the known line equations (Eq. 4 and 6) and are calculated as follows:

$$z_1 = m_1 x + b_1 \tag{4}$$

$$\arctan(m_1) = \beta \tag{5}$$

$$z_2 = m_2 x + b_2 \tag{6}$$

$$\arctan(m_2) = \alpha \tag{7}$$

The distance Z to the work surface also need to be corrected and can be calculated using the term b of the line equation Z_1 and is better explained in the Santos *et al.* (2018) paper in chapter 2 item C. The following equation 8 is used to calculate Z_d:

$$z_{ref} - b_1 = Z_d \tag{8}$$

2.2 Experiment

In order to test and guarantee if the algorithms could achieve the perpendicularity accuracy, a Design of Experiment (DoE) was implemented considering the requirement of 0.5^{o} maximum deviation between the side face of the sensor and the surface, similarly to the work described on Santos *et al.* (2018). Even though the observations made are almost the same, it is important to mention some of them again:

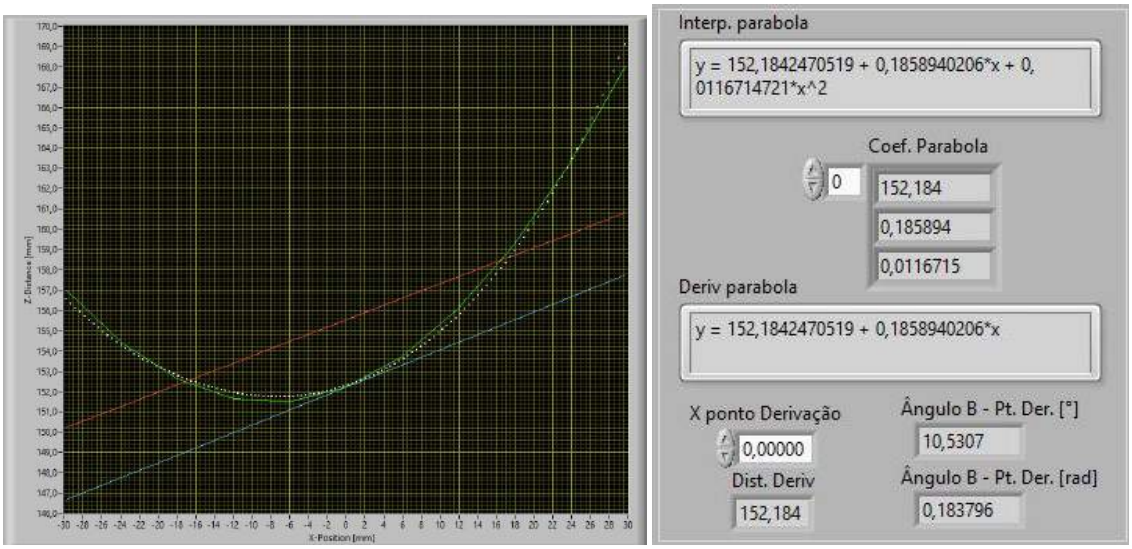

(a) Point cloud acquired by scan sensor and plotted equations. (b) Parabola equations.

Figure 6: Correction angles on curved surfaces.

- Since all the runs of the experiment were made under similar conditions, it is assumed that the climatic factors do not interfere the factors of interest;
- The maximum error admitted by the algorithm is 0.1^{o} and there is also a 10-iteration limit. If the limit is reached, the error is compared to the requirement of 0.5^{o};
- In order to maintain the reliability, the order between the methods were randomized;
- In each run of the test, the target surface and the scan sensor face were scanned using the laser tracking system for the purpose of orientation error calculation as shown on Fig. 7.

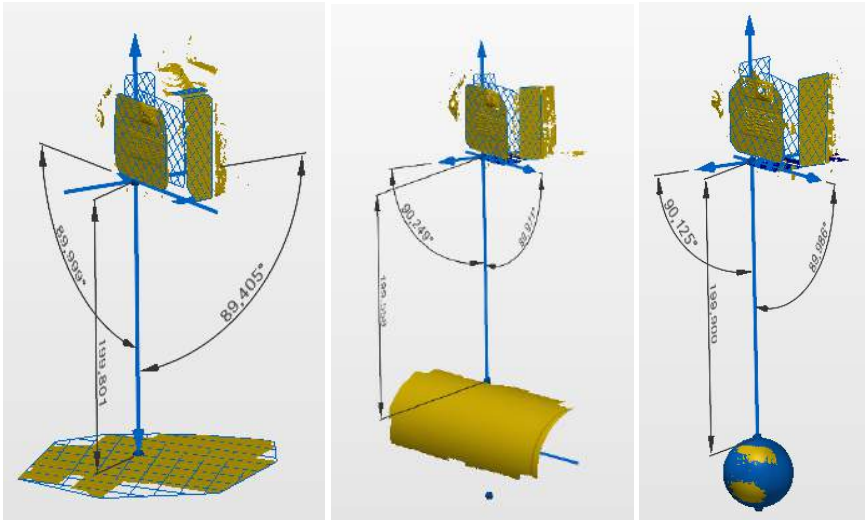

(a) Poly Works Flat Surface Analysis. (b) Poly Works Tubular Surface Analysis. (c) Poly Works Spherical Surface Analysis.

Figure 7: Poly Works Analysis.

For the analysis, the experiment chosen was a simple factorial for the flat and tubular surface, with the only factor being the "perpendicularity" with two levels, each referencing the used method, Parabolic Static or Semi Static. For the

spherical surface, as there were not two different methods to be applied, a single sample Z-Test was chosen as it is enough to prove the applicability of the single method tested. The proposed hypothesis are shown as follows, in equations 9, 10 for the flat and tubular surfaces and in equations 11, 12 for the spherical surface.

$$H0 : \mu_1 = \mu_2 \tag{9}$$

$$H1 : \mu_1 \neq \mu_2 \tag{10}$$

where the μ_1 is the Parabolic Static Method mean, while μ_2 is the mean of Semi-Static Method.

$$H0 : \mu > 0.5^{\circ} \tag{11}$$

$$H1 : \mu \leq 0.5^{\circ} \tag{12}$$

The considered statistical model used on the flat and on the tubular surface is represented in equation 13, and for the spherical surface in equation 14.

$$Y_{ij} = \mu + A_i + E_{ij} \tag{13}$$

$$Y_k = \mu + E_k \tag{14}$$

where i is the i-th factor level of the method, j and k are the number of replicates of each experiment. Y_{ij} and Y_k are the resulting deviation angle from the flat and tubular surface and spherical surface, respectively. While on the right side of the equation, μ represents the overall mean of Y, A_i is the influence of the $i - th$ utilized method, E_{ij} and E_k are the random error.

The final variable (deviation angle phi) was obtained by calculating the resultant (eq. 15) of two ortogonal vectors found by the methods and measured using the LEICA system (Fig. 4).

$$\phi = \sqrt{\alpha^2 + \beta^2} \tag{15}$$

3. RESULTS

The results of the experiment described on the last section will be separated in three parts, each one referencing the different surfaces used to evaluate the algorithms. All the results summarized in the tables were obtained through the results of the 3D model provided by the measurement using the LEICA Scan, and analysed with the Polyworks CAD software. All three parts were analyzed with the statistic software R, but the first two parts, the flat and the tubular surface used the analysis of variance method, ANOVA (Montgomery, 2017), while the spherical surface used a single-sample Z-Test approach, as there is only one level in a single factor, and the only verification was to assure the method satisfied the 0.5 degrees of perpendicularity maximum deviation.

3.1 Flat Surface

The static method data on table 1 was not obtained from the same batch of measurements. Instead, is the same as Santos *et al.* (2018), since the system, equipment and application are similar. In table 1 StMe is a short for Parabolic Static-Method and SE is Semi-Static Method

Table 1: Measurements for angle deviation for Flat Surface

Method	Replicates					
	1	2	3	4	5	6
StMe	0,196	0,215	0,112	0,185	0,178	0,147
SE	0,513	0,340	0,444	0,572	0,527	0,488

The first analysis of the data is shown on Fig. 8, indicating a clear difference between methods, and that hypothesis is confirmed by the ANOVA, summarized on Fig. 9. The P-Value being smaller than the default confidence level for aeronautics of 1% represents that the null hypothesis, that both methods are equals, is rejected.

To assure the normality of the used data, guaranting it is a valid despite the fact different methods data were acquired on different days, it was plotted the residues normality graph (Fig. 10a), followed along with the Shapiro-Wilk test(Fig. 10b). If the scattered points on the graph resembles a straight line, it can be graphically affirmed that the residual is normal. The null hypothesis of the Shapiro-Wilk test is that the residues are normal, therefore confirmed by the P-Value of 0.4115, greater than the confidence level of 0.01.

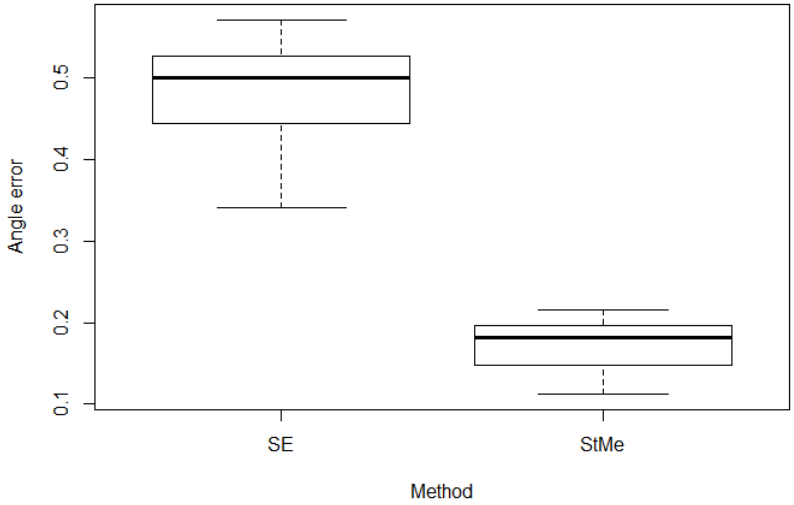

Figure 8: Boxplot Flat Surface

```
             Df  Sum Sq Mean Sq F value   Pr(>F)
factorMethod  1 0.28576 0.28576   72.69 6.71e-06 ***
Residuals    10 0.03931 0.00393
---
Signif. codes:  0 ‘***’ 0.001 ‘**’ 0.01 ‘*’ 0.05 ‘.’ 0.1 ‘ ’ 1
```

Figure 9: ANOVA Flat Surface

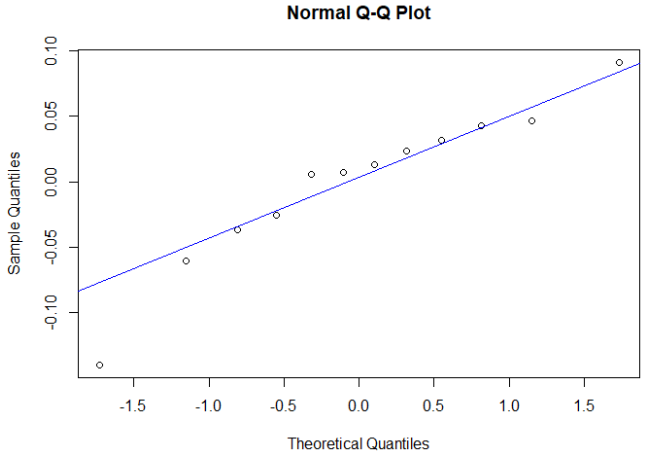

(a) Normality Flat Surface.

```
        Shapiro-Wilk normality test

data:  res
W = 0.93287, p-value = 0.4115
```

(b) Shapiro-Wilk Flat Surface.

Figure 10: Flat Surface normality test.

3.2 Tubular Surface

Similar to the flat surface, the analysis on the tubular surface will follow exactly the same steps, analyse the boxplot, running the ANOVA and verifying the residues of the data with the normality plot and Shapiro-Wilk test. The summarized data for the tubular surface is represented on table 2, followed by the boxplot graph on Fig. 11.

Table 2: Measurements for angle deviation for Tubular Surface

Method	Replicates					
	1	2	3	4	5	6
StMe	0,575	0,844	0,855	0,765	0,717	0,806
SE	0,090	0,250	0,264	0,047	0,114	0,235

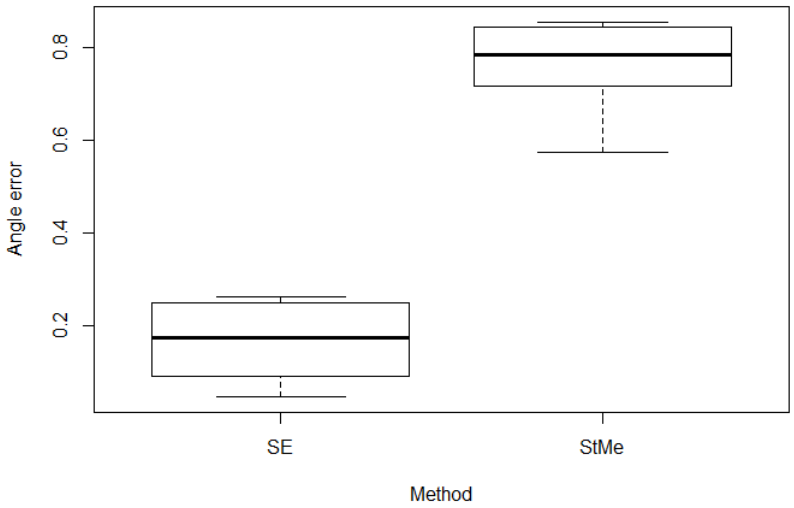

Figure 11: Boxplot Tubular Surface

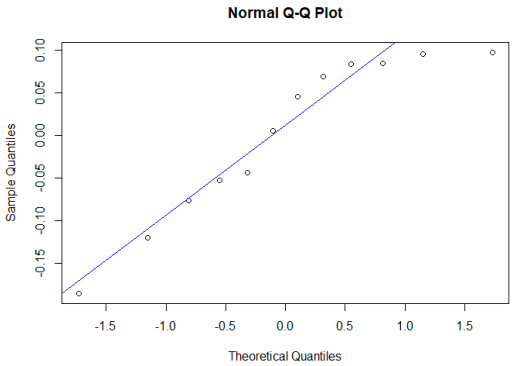

(a) Normality of Tubular Surface.

```
        Shapiro-Wilk normality test

data:  res
W = 0.89533, p-value = 0.1381
```

(b) Shapiro-Wilk Tubular Surface.

Figure 12: Tubular Surface normality test.

Analysing the boxplot, it is possible to conclude that the parabolic static method (StMe) is not appropriate for curved surfaces, as foreseen in Santos *et al.* (2018), as it failed to satisfies the 0.5 degrees limit deviation. On the other hand, the semi static method graphically satisfied the fore mentioned limit deviation, being unnecessary further analysis. The normality graph of the tubular data is shown on Fig. 12a and the Shapiro-Wilk results are summarized in Fig. 12b. The P-Value greater than 1% proves the normality of the residues.

3.3 Spherical Surface

The analysis procedure for the spherical surface differs from the others, as there is no different methods to compare, and it is only needed to assure that the method satisfies the maximum deviation limit of 0.5 degrees. The boxplot represented in Fig. 13a shows that the median deviation is close to 0.1 degrees, but there is also an outlier. Running the single-sample Z-test (Montgomery, 2017) the summarized result is shown on Fig. 13b. Analysing the result from the one-sample Z-test, the P-Value indicates that the null hypothesis should be reject (smaller than the confidence level), assuring the that the measurements would have the deviation smaller than the maximum limit of 0.5 degrees.

Finalizing the analysis, we also checked the normality graph (Fig. 14a) and executed the Shapiro-Wilk test (Fig. 14b)


```
        One-sample z-Test

data:  Angle
z = -16.173, p-value < 2.2e-16
alternative hypothesis: true mean is less than 0.5
```

(a) Boxplot Spherical Surface. (b) Z-Test Spherical Surface.

Figure 13: Z-test Spherical results.

using the angle data. The P-Value obtained from the Shapiro-Wilk test proved all the residues from the data are normal, thus validating the experiment.

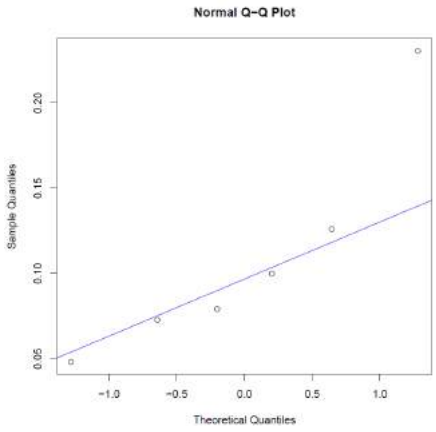


```
        Shapiro-Wilk normality test

data:  Angle
W = 0.85314, p-value = 0.1669
```

(a) Normality Spherical Surface. (b) Shapiro-Wilk Spherical Surface.

Figure 14: Spherical Surface normality test.

4. CONCLUSION

This paper showed the studies that followed Santos *et al.* (2018), and used a new approach based on the Static Method, called Parabolic Static Method, on curved surfaces to evaluate its effectiveness. Beside that, it was introduced a new method, now called semi-static, that uses only the scan sensor as reference and rotates the end-effector 90 degrees on the Z_s axis (Scan Sensor frame) to obtain two lines necessary for the calculation.

The semi-static method was tested on a flat surface so the results could be compared to the previous results obtained by the static method on the same surface (Santos *et al.*, 2018). In this case, the static method proved to be better than the semi-static, as the semi-static did not guaranteed to achieve the maximum deviation of 0.5^o. A possible cause for this error is the same stated in Santos *et al.* (2018), which is an additional source of error: The robot movement that is executed for measuring during the method. Despite the failure on the flat surface, the semi-static achieved acceptable results during the tests with the tubular surface, performing better than the static method. This result is probably because the static method can not accurately fit a curved surface in one direction due to the lack of a point to interpolate the parabola in the direction concurrent with the scan sensor. On the spherical surface, the only applied method, the semi static, proved to be reliable, since the results given by the Z-Test shows that the deviation angle is less than the 0.5^o limit.

5. ACKNOWLEDGEMENTS

This work is related to the projects of the Centro de Competência em Manufatura(CCM), under development at Instituto Tecnológico de Aeronáutica(ITA), in partnership with Embraer and supported by FINEP, CAPES and CNPq.

6. REFERENCES

Cibiel, C., Redman, M. and Prat, P., 2006. "Automation for the assembly of the bottom wing panels on stringers for the a320". Technical report, SAE Technical Paper.

Furtado, L.F.F., Villani, E. and Sutério, R., 2009. "A perpendicularity measurement system for industrial robots". In *Proc. of the 20th International Congress of Mechanical Engineering (COBEM)*.

Gao, Y., Wu, D., Dong, Y., Ma, X. and Chen, K., 2017. "The method of aiming towards the normal direction for robotic drilling". *International Journal of Precision Engineering and Manufacturing*, Vol. 18, No. 6, pp. 787–794.

Gao, Y., Wu, D., Nan, C. and Chen, K., 2015. "Normal direction measurement in robotic drilling and precision calculation". *The International Journal of Advanced Manufacturing Technology*, Vol. 76, No. 5-8, pp. 1311–1318.

Liu, J., Shao, X., Liu, Y., Liu, Y. and Yue, Z., 2007. "The effect of holes quality on fatigue life of open hole". *Materials Science and Engineering: A*, Vol. 467, No. 1-2, pp. 8–14.

Montgomery, D.C., 2017. *Design and analysis of experiments*. John wiley & sons.

Santos, K.R.d.S., de Carvalho, G.M., Tricarico, R.T., Ferreira, L.F.L.R., Villani, E. and Sutério, R., 2018. "Evaluation of perpendicularity methods for a robotic end effector from aircraft industry". In *2018 13th IEEE International Conference on Industry Applications (INDUSCON)*. IEEE, pp. 1373–1380.

7. RESPONSIBILITY NOTICE

The authors are the only responsible for the printed material included in this paper.